A Generalized Green-Function Method for Wave Field Analysis

Hitoshi Nishimura [1], Michio Matsuoka [2] and Akira Matsumoto [3]

Abstract

The Green-function method for analyzing wave refraction, diffraction and reflection is improved by deriving rational explicit formulations of boundary conditions. Possibilities and limitations of the method are discussed. Trial computations and their comparisons with experiments demonstrate the validity and usefulness of the numerical model.

Introduction

To analyze refraction, diffraction and reflection of simple sinusoidal waves is one of the very fundamental problems in the field of coastal engineering. If an accurate and simple method is provided for this purpose, deformation of irregular waves may also be analyzed through superposition of solutions for constituent waves. In this context, numerical modeling based on the Green-function method is quite promising since it describes the diffraction and multiple reflection of waves more accurately than any other methods. This kind of numerical model was first proposed by Barailler and Gaillard (1967), and has been widely used in particular for simulation of waves in semi-closed sea basins. In numerical models presently used, however, continuation of solutions are often insufficient at artificial boundaries.

In the following sections, rational explicit formulations of boundary conditions is· derived for more rigorous computation of two-dimensional wave fields. Validity of the numerical model thus improved is examined through trial computations and their comparisons with experiments.

---

[1]Professor, Inst. of Eng. Mech., Univ. of Tsukuba., Tsukuba, Ibaraki, 305, Japan.

[2]Senior Researcher, Applied Hydraulic Laboratory, Nippon Tetrapod Co., Ltd., 2-7 Nakanuki, Tsuchiura, Ibaraki, 300, Japan.

[3]Ditto.

Principle of the Green-Function Method

If we express the wave profile $\zeta(x, y, t)$ in a water area with a uniform depth as

$$\zeta = f(x, y) \cdot e^{i\omega t} \tag{1}$$

the complex amplitude $f(x, y)$ satisfies the following Helmholtz equation:

$$\frac{\partial^2 f}{\partial x^2} + \frac{\partial^2 f}{\partial y^2} + k^2 f = 0 \tag{2}$$

where (x, y) is the Cartesian coordinate in a horizontal plane, t is the time, ω is the angular frequency, and k is the wave number.

Suppose the existence of a perfectly reflective wall along the x-axis and a wave source at a point (ξ, η), as shown in Fig.1. It is well known that the resulting wave field in the semi-finite region of $y > 0$ is then

$$f(x, y) = -\frac{i\Gamma}{4}[H_0^{(1)}(kr^+) + H_0^{(1)}(kr^-)] \tag{3}$$

$$r^\pm = \sqrt{(x - \xi)^2 + (y \mp \eta)^2} \tag{4}$$
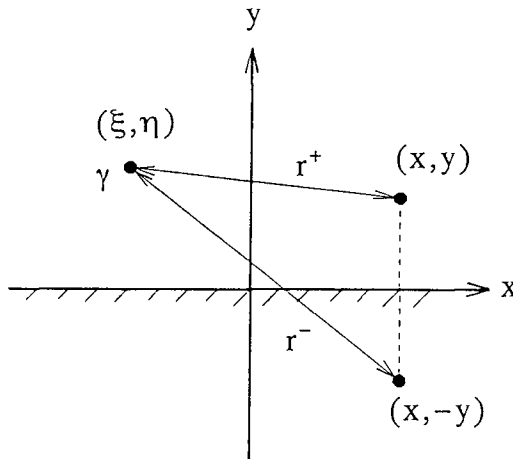
Figure 1: Definition sketch.

in which $H_0^{(1)}$ denotes the zeroth-order Hankel function of the first kind. Note that the complex source intensity Γ represents the wave phase as well as the amplitude. The solution (3) satisfies the basic equation (2) and, at the same time, the boundary condition $\partial(f_1 + f_2)/\partial y = 0$ along the x-axis. It also satisfies Sommerfeld's radiation condition toward the infinity.

For a particular case that the wave source is located on the x-axis ($\eta = 0$), the expressions (3) and (4) are simplified as follows:

$$f(x,y) = -\frac{i\Gamma}{2} H_0^{(1)}(kr) \tag{5}$$

$$r^{\pm} = \sqrt{(x - \xi)^2 + y^2} \tag{6}$$

Distribution of such wave sources along the boundary of a water area will cause a composite wave field, which is expressed by the integration of the unit solution:

$$f(x,y) = \int_C \gamma(s) \cdot H_0^{(1)}(kr) \, ds \tag{7}$$

where s is the coordinate taken along the boundary C, r is the distance from the boundary point (s) to the point (x,y), and $\gamma(s)ds$ corresponds to the wave source intensity Γ in Eq.(5). The wave source distribution has to be determined so that the resulting wave field satisfies all the boundary conditions imposed, as correctly suggested by Lee (1969, 1971) for harbor oscillation analysis.

Relationship between the Source Intensity and Wave Amplitude on a Boundary

Consider the situation that wave sources in the semi-infinite region of $y > 0$ produce a wave field $f_1(x,y)$. As to the waves propagating across the x-axis, the following relationship proves from Green's theorem between the complex amplitude and its gradient in the y-direction:

$$f_1(x,0) = -\frac{i}{2} \int_{-\infty}^{\infty} \left. \frac{\partial f_1(\xi,\eta)}{\partial \eta} \right|_{\eta=0} \cdot H_0^{(1)}(k\,|x - \xi|) \, d\xi \tag{8}$$

On the other hand, a similar relationship is obtained for a wave field $f_2(x,y)$ which is produced in the same region by the source distribution $\gamma_2(x)$ along the x-axis:

$$f_2(x,y) = -\frac{i}{2} \int_{-\infty}^{\infty} \left. \frac{\partial f_2(\xi,\eta)}{\partial \eta} \right|_{\eta=0} \cdot H_0^{(1)}(kr) \, d\xi \tag{9}$$

It can thus be concluded that the source intensity is directly proportional to the local gradient of resulting wave amplitude in the normal direction to the boundary:

$$\gamma_2(\xi) = -\frac{i}{2}\frac{\partial f_2(\xi,\eta)}{\partial \eta}\bigg|_{\eta=0} \tag{10}$$

Condition of Reflective Boundary

If x-axis is a perfectly reflective boundary in the above discussion, then the incident waves $f_1(x,y)$ and reflected waves $f_2(x,y)$ appear in the semi-infinite region. The boundary condition in this case is

$$\frac{\partial(f_1+f_2)}{\partial y}\bigg|_{y=0} = 0 \tag{11}$$

which leads to the following simple expression of the source intensity:

$$\gamma_2(\xi) = -\frac{i}{2}\frac{\partial f_2(\xi,\eta)}{\partial \eta}\bigg|_{\eta=0} \tag{12}$$

In rigorously formulating a condition of partial reflection, hydraulic mechanism of wave reflection has to be known. A conventional method for simulating the partial reflection is to simply reduce the source intensity by multiplying the reflection coefficient β as follows:

$$\gamma_2(\xi) = -\frac{i\beta}{2}\frac{\partial f_1(\xi,\eta)}{\partial \eta}\bigg|_{\eta=0} \tag{13}$$

Continuation of Solutions along an Open Boundary

For the convenience of numerical computation, the whole region in question is often divided into subregions by supposing imaginary boundaries between them. A breakwater gap illustrated in Fig.2 is a typical example of such a boundary. In the figure, waves $f_I(x,y)$ are incident to the imaginary boundary C on the x-axis. Note that $f_I(x,y)$ represents all the incident waves to C including those from the boundaries immediately beside C.

If the boundary is either finite or semi-infinite, waves are partly reflected as they are transmitted across the boundary. In other words, two kinds of wave sources are in general to be distributed along a transmissive boundary. On one side of the boundary, the reflected waves $f_R(x,y)$ is superposed on the incident waves $f_I(x,y)$, whereas only transmitted waves $f_T(x,y)$ propagate on the other side. It is thus feasible for these two wave fields to coincide in terms of both the amplitude and its gradient along the boundary C:

$$(f_I + f_R)\big|_C = f_T\big|_C \tag{14}$$

$$\frac{\partial(f_I + f_R)}{\partial y}\bigg|_C = \frac{\partial f_T}{\partial y}\bigg|_C \tag{15}$$

These conditions lead to the following integral equations for the source intensities γ_R and γ_T for reflected and transmitted waves respectively:

$$2\int_C \gamma_R(\xi) \cdot H_0^{(1)}(k\,|x - \xi|)\,d\xi = f_I^*(x,0) - f_I(x,0) \tag{16}$$

$$2\int_C \gamma_T(\xi) \cdot H_0^{(1)}(k\,|x - \xi|)\,d\xi = f_I^*(x,0) + f_I(x,0) \tag{17}$$

where

$$f_I^*(x,0) = -\frac{i}{2}\int_C \frac{\partial f_I(\xi,\eta)}{\partial \eta}\bigg|_{\eta=0} \cdot H_0^{(1)}(k\,|x - \xi|)\,d\xi \tag{18}$$

and

$$f_R(x,y) = \int_C \gamma_R(\xi) \cdot H_0^{(1)}(kr)\,d\xi \tag{19}$$

$$f_T(x,y) = \int_C \gamma_T(\xi) \cdot H_0^{(1)}(kr)\,d\xi \tag{20}$$

For solution of the above equations, they are discretized by dividing the boundary into a number of segments. The problem is then ascribed to linear systems of simultaneous equations, and the source intensities are obtained through matrix operations. Since the coefficient matrices of the systems are fixed for each boundary of this type regardless of wave conditions, inverse matrices once calculated can be repeatedly used throughout the computation.
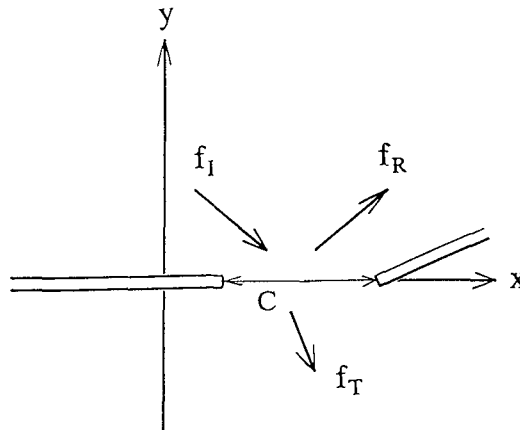
Figure 2: Imaginary boundary.

In the actual computation, it is not necessary to solve both the above equations. After solving one of them for γ_R or γ_T, we can easily evaluate the other from the following relationship:

$$\gamma_I(x) + \gamma_R(x) + \gamma_T(x) = 0 \tag{21}$$

Even if incident waves with uniform amplitude are incident to the boundary, wave sources thus obtained are not uniform with high peaks at the boundary ends. These peaks represent the singularity of the boundary ends, reproducing fields of diffracted waves with good approximation. It is important to note here that the source intensity cannot necessarily be related to the local energy density of incident waves.

Outline of the Numerical Model

When the configuration of a sea area in question is complicated, the whole region for computation is divided into several convex polygonal subregions. A semi-infinite open sea area is regarded as one of the subregions. The other subregions are totally enclosed by boundaries, at least one of them being transmissive. All the boundaries are subdivided into a number of segments and the effect of each segment is represented by a wave source. A transmissive boundary serves as two boundaries at once for two subregions on its both sides, where two sources defined are for either reflected or transmitted waves depending on the subregion currently treated.

The distribution of source intensities is calculated for each boundary. The flow of computation starts from the the subregion of wave incidence. It moves from one subregion to the next, and from one boundary to another in a subregion. Since the source intensities are interdependent, these boundarywise calculations over the whole region are repeated until all the intensities reach an equilibrium.

It is somewhat difficult to formulate the condition of a partially transmissive boundary. Such a boundary may be reasonably regarded as a fully reflective boundary in evaluating reflected waves, and as a fully open boundary for transmitted waves. Prior to these calculations, the incident wave amplitudes are to be reduced by multiplying reflection or transmission coefficient. In this case, the source intensities for reflected and transmitted waves have to be memorized separately on both the sides of the boundary.

The present method for wave field analysis can be applied even to a water area with arbitrary bathymetry by numerically obtaining unit solutions to replace the Hankel function. For the calculation of unit solutions, a relatively simple method for analyzing wave refraction may be employed, since the main part of wave diffraction is included in principle in the process of superposition of point source waves. Nonlinear wave deformation, however, can never be analyzed by means of the Green-function approach as it is essentially based on the superposition of unit solutions.

Physical Model Experiments

A series of experiments on waves in a harbor were conducted (Photo 1) to provide wave distribution data to examine performance of the numerical model described above. The model harbor configuration shown in Fig.3 and experimental conditions listed in Table 1 were determined along one of the model cases specified for trial simulation works by a subcommittee of the Coastal Engineering Conference, JSCE. The model was installed on a horizontal bed in a narrow wave basin. Gaps between the harbor and basin walls were filled by wave absorbing material to avoid the elevation of the mean water level.

In some cases of the experiments, tetrapod mounds were arranged on the outer sea sides of the breakwaters, but all the other walls were vertical walls. As a matter of fact, arrangement of absorbing facility inside the harbor significantly narrows the harbor area in such a small-scale model. The reflection coefficient for each part of the model was separately estimated by applying Healy, Goda (1976) and Isaacson's (1991) methods, as summarized in Table 2.

Wave heights were measured using servo-type gauge array at every 10cm grid point over the whole area near and inside the harbor. The measurements were repeated more than twice for each case, but no significant scattering was observed in the data obtained. The incident wave heights listed in Table 1 were obtained at the location of the harbor entrance prior to the model installation.

Photo 1: Experimental setup.
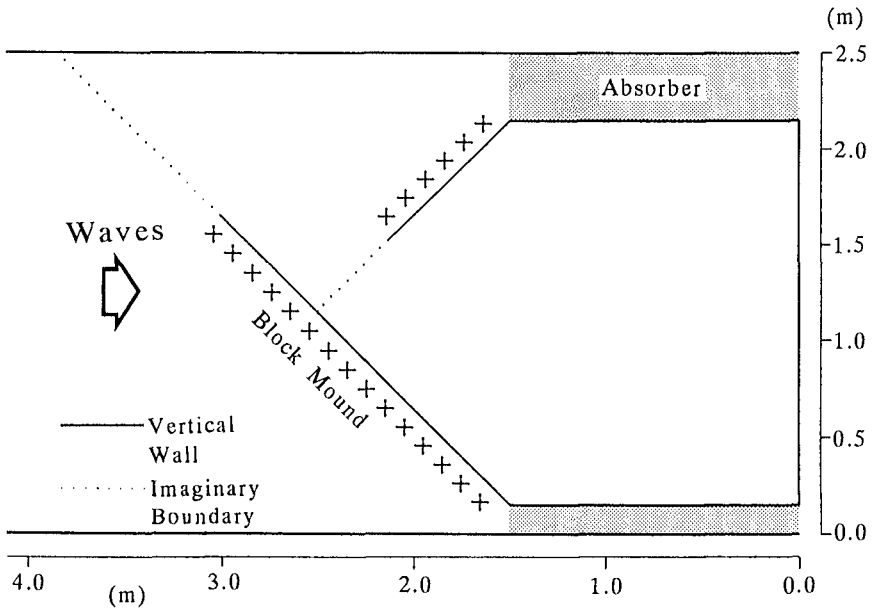
Figure 3: Experimental setup.

Table 1: Experimental conditions.

Case	Water depth (cm)	Period (s)	Incident wave height (cm)	Breakwaters
1	12.0	0.70	2.62	with block mounds
2	12.0	0.72	2.06	with block mounds
3	12.0	0.70	1.96	without block mounds

Table 2: Reflection coefficient.

	Measured value	For computation
Vertical wall	0.95-1.00	0.95
Block mound	0.35-0.40	0.40
Wave absorber	0.30-0.35	0.30

Comparison of Numerical Computations and Experiments

In the numerical computations, the whole region was divided into four subregions. Two imaginary boundaries are shown in by dotted lines in Fig.3. Another boundary for wave incidence was assumed at 4m from the outer breakwater tip, and further offshore area was treated as a semi-infinite region. All the boundaries were divided into segments with length of roughly 1/20 wavelength. The reflection coefficient values used are also shown in Table 2, and the boundarywise computations were repeated until the relative accuracy of 1/1000 at maximum was attained.

Figure 4 compares measured and calculated distributions of relative wave heights normalized with the incident wave height for Case-1 with a period of 0.70s. The numerical model well simulates the field of standing waves formed inside the harbor, although the wave heights calculated are somewhat smaller than those measured. The incident wave height may have been substantially increased involving reflected waves from the wave generator. In numerical analyses, waves in the innermost area of the harbor are apt to be underestimated as they are subject to multiple diffractions. This sort of tendency, however, is not apparent at all here.

Figure 5 presents a similar comparison for Case-2 with a slightly longer period of 0.72s. It is seen that the wave period sensitively affect the wave field in such a system of multiple reflection, as is well simulated by the numerical model. These periods may be close to one of the resonant oscillation periods of the harbor water.

The effects of the absorbing mounds on the breakwater fronts first appears on the wave height distribution outside the harbor. Then the change in wave heights along the harbor entrance indirectly influences the wave field inside the harbor. Figure 6 shows wave fields for Case-3, where the block mounds were eliminated. The computation again reasonably reproduces significant differences in the wave height distribution which is noticed through comparison with Fig.4 for the Case-1 experiment.

Concluding Remarks

The Green-function method provides a powerful tool for analyzing wave diffraction and multiple reflection of coastal and harbor waves. The rational treatment of imaginary boundaries allows the arbitrary division of water area with a complicated configuration without deteriorating the accuracy of total computation. The present model is rather simple and minimizes empirical factors for its actual application.

Since computer memory and computational labor required are not so large, even irregular waves can be treated so far as the linear superposition of constituent waves are acceptable. The model may be extended for arbitrary bathymetry, but cannot contribute to analyses of nonlinear wave deformation.
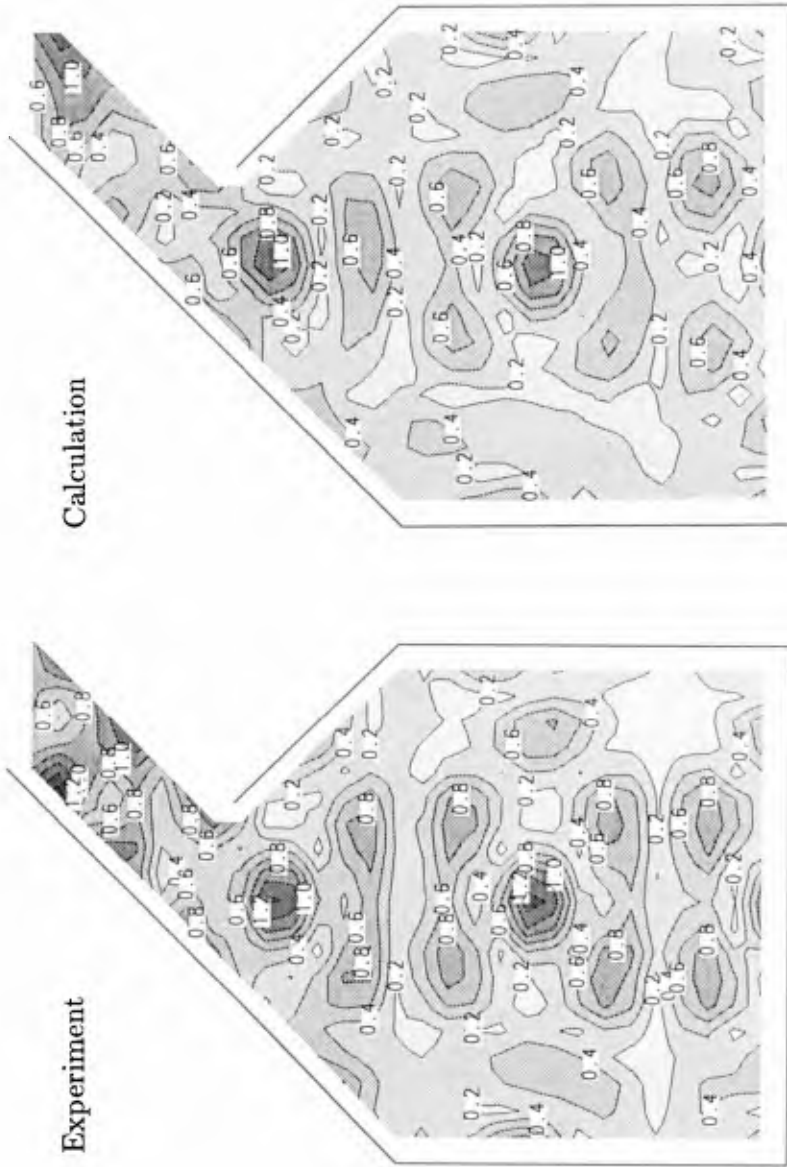
Fig. 4: Relative wave height distribution (Case 1, period: 0.70s).
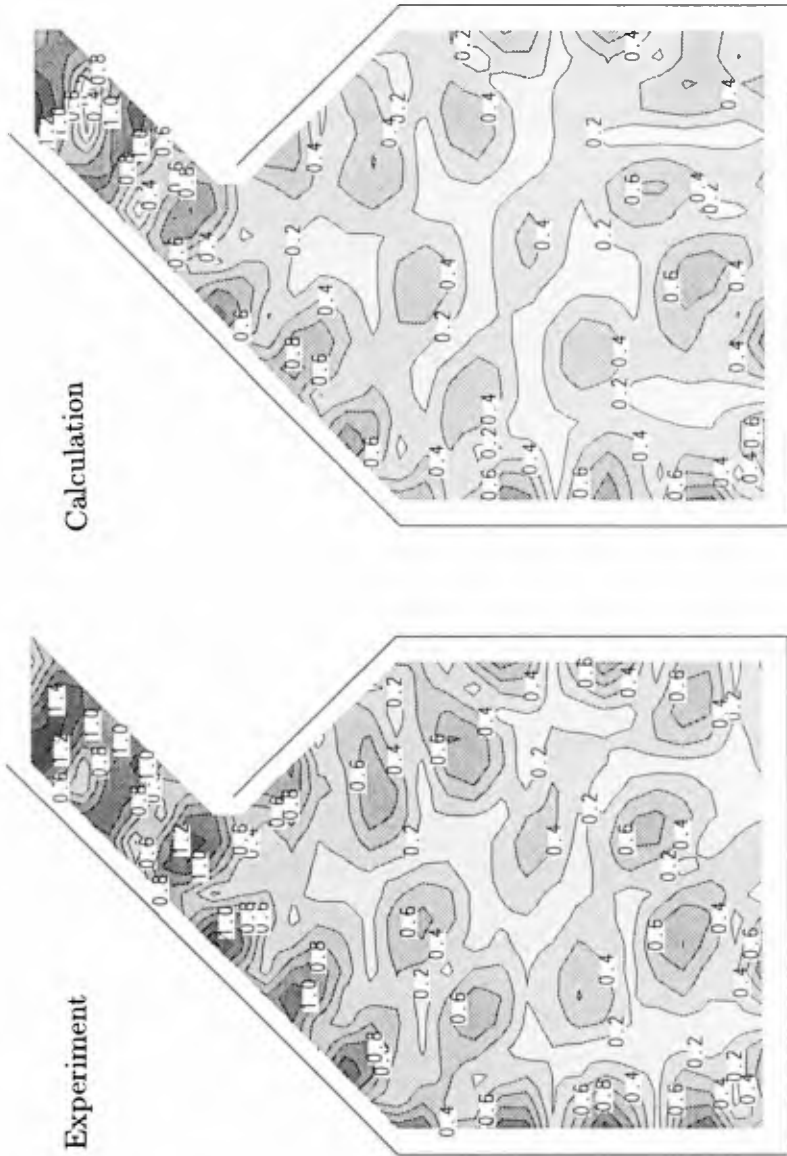
Fig. 5: Relative wave height distribution (Case 2, period: 0.72s).
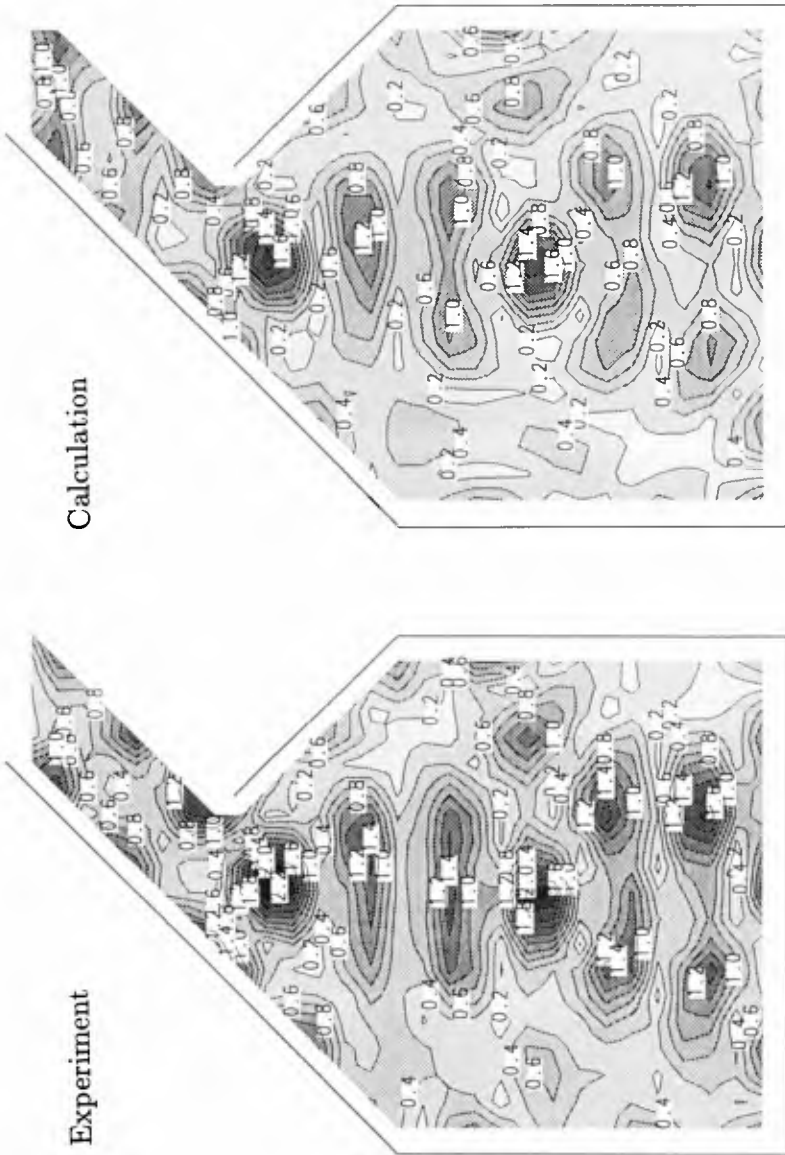
Fig. 6: Relative wave height distribution (Case 3, period: 0.70s, without block mounds).

Acknowledgment

References

Barailler, L., and P. Gaillard (1967). Évolution récente des modèles mathématiques dagitation due à la houle. La Houile Blanche, Vol.22, No.8, pp.861-869.

Goda, Y. (1976). Estimation of incident and reflected waves in random wave experiments. Tech. Note of Port and Harbour Res. Inst., Min. of Transport, Japan, No.248, 24p. (in Japanese)

Isaacson, M (1991). Measurement of regular wave reflection, J. Waterway, Port, Coastal and Ocean Eng., ASCE, Vol.117, pp.553-509.

Lee, J.-J., and F. Raichlen (1969). Wave induced oscillations in harbors of arbitrary shape. W. M. Keck Lab., Calif. Inst. of Tech., Rep. No.KH-R-20, 266p.

Lee, J.-J., and F. Raichlen (1971). Wave induced oscillations in harbors with connected basins. W. M. Keck Lab., Calif. Inst. of Tech., Rep. No.KH-R-26, 135p.